

Zero-shot Object-Centric Instruction Following: Integrating Foundation Models with Traditional Navigation

Sonia Raychaudhuri^{1,2}, Duy Ta¹, Katrina Ashton^{1,3}, Angel X. Chang², Jiuguang Wang¹, Bernadette Bucher^{1,4}

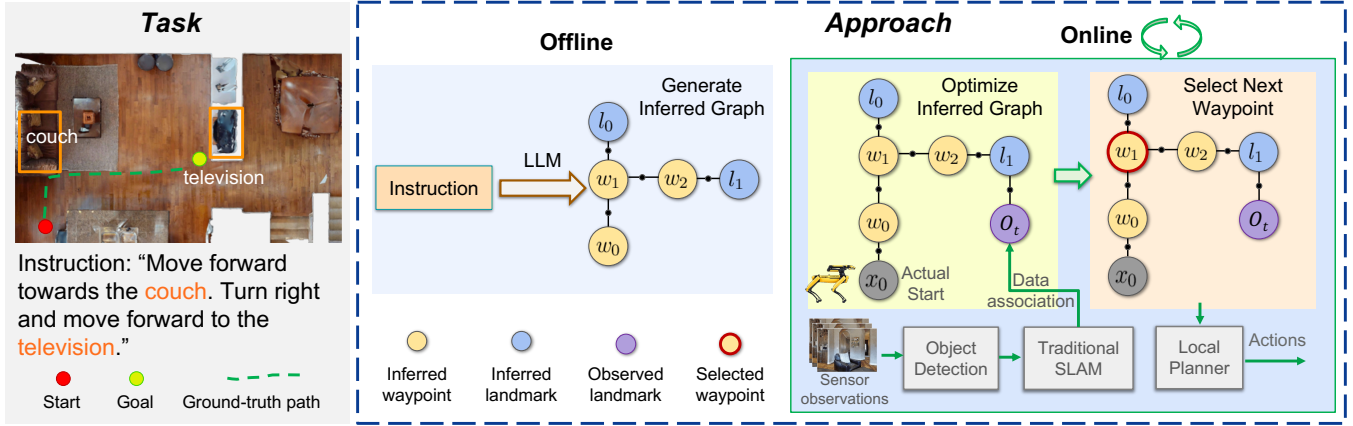


Fig. 1: The robot is tasked with following a language instruction in an unseen environment to reach the final target (left). We introduce *Language-Inferred Factor Graph for Instruction Following* (LIFGIF) (right), a novel method that infers a graph from the instruction using an LLM, offline, and thereafter optimizes the graph with actual observations at every step, online, during navigation. The robot selects the next waypoint from the inferred graph and moves toward it using a local planner.

Abstract—Large scale scenes such as multifloor homes can be robustly and efficiently mapped with a 3D graph of landmarks estimated jointly with robot poses in a factor graph, a technique commonly used in commercial robots such as drones and robot vacuums. In this work, we propose *Language-Inferred Factor Graph for Instruction Following* (LIFGIF), a zero-shot method to ground natural language instructions in such a map. LIFGIF also includes a policy for following natural language navigation instructions in a novel environment while the map is constructed, enabling robust navigation performance in the physical world. To evaluate LIFGIF, we present a new dataset, Object-Centric VLN (OC-VLN), in order to evaluate grounding of object-centric natural language navigation instructions. We compare to two state-of-the-art zero-shot baselines from related tasks, Object Goal Navigation and Vision Language Navigation, to demonstrate that LIFGIF outperforms them across all our evaluation metrics on OC-VLN. Finally, we successfully demonstrate the effectiveness of LIFGIF for performing zero-shot object-centric instruction following in the real world on a Boston Dynamics Spot robot. sonia-raychaudhuri.github.io/nlslam.

I. INTRODUCTION

Robotics studying mapping and navigation have developed methods for creating landmark maps from visual observations and using those maps for autonomous navigation [1]–[7]. In fact, work in this area has matured far

enough to move beyond the research community. Landmark-based mapping and navigation systems are widely used for autonomous robot operation in many industry applications, including home robot vacuum cleaners [8], [9] and drones for surveying and inspection [10]. With recent advances in natural language understanding due to large language and vision-language models [11]–[15], the next frontier is to determine how to accurately align natural language navigation instructions with observation-based autonomous decision making capabilities in these mature robotic systems. Effective alignment of this information could enable many new robotic capabilities including natural language instruction following.

To support research in this direction, researchers have developed benchmarks for evaluating an autonomous agent's ability to follow natural language navigation instructions in simulation, specifically R2R [16], RxR [17], and VLN-CE [18]. These benchmarks consist of datasets of natural language instructions and associated paths through scanned Matterport 3D scenes of residential homes [19]. The language instructions in these datasets contain both object-centric references to landmarks ('move forward to the *blue chair*, turn left and stop at the *wooden table*') and relative positional references to the current agent position ('move forward and turn left and stop in the hallway'). Methods addressing these tasks are largely trained on data in simulation and struggle to generalize to the real world [20], [21].

Contributions. In this work, we introduce *Language-Inferred Factor Graph for Instruction Following* (LIFGIF), a

¹Work done during SR and KA's internships. SR, DT, KA, JW and BB are with the Robotics and AI Institute {dta, jw}@rai-inst.com

²SR and AC are with Simon Fraser University {sraychau, angelx}@sfu.ca

³KA is with University of Pennsylvania {kashton}@upenn.edu

⁴BB is with University of Michigan {bucherb}@umich.edu

novel method for grounding natural language instructions to landmarks and robot poses in a factor graph, while performing zero-shot navigation in unseen unexplored environments. Our approach avoids previous limitations to performing instruction following robustly in the physical world by building off of robust mapping and navigation techniques for autonomous robots. In addition, LIFGIF leverages pre-trained vision and language foundation models and requires no task-specific training. We demonstrate the viability of LIFGIF to successfully perform real-world instruction following on a Boston Dynamics Spot robot.

We are interested in achieving *alignment* between natural language instructions and a widely-used landmark-based map structure in robotics as well as natural language navigation instruction following. To support both of these goals, we introduce a novel dataset, *Object-Centric VLN* (OC-VLN), of object-centric navigation instructions. In this dataset, we ensure that the navigation instructions include references to landmarks which compose our sparse 3D map. We compare our method, LIFGIF, to two state-of-the-art zero-shot baselines from related tasks, Object Goal Navigation and Vision Language Navigation, to demonstrate that LIFGIF outperforms them across all our evaluation metrics on OC-VLN.

II. RELATED WORK

Natural Language Grounding to Landmarks. Recently there has been much interest in fusing information from 2D foundation models into 3D scene representations. Many approaches represent per-pixel semantic features using explicit representations such as pointclouds [22]–[25], or implicit neural representations [26]–[37]. For methods which plan over objects instead of dense features, such scene representations necessitate extra storage and computation compared to object-centric representations. More similar to our approach, some methods [5], [38], [39] use a 3D scene graph (3DSG) where nodes and edges represent objects and inter-object relationships, respectively. Unlike us, however, these methods require constructing a dense 3D representation of the scene and some also do not consider pose uncertainty [38], [39]. Also, unlike us, none of these approaches incorporate prior information about the scene.

Object Navigation. Navigation in unseen unstructured environments is a key challenge in robotics and AI. Research spans from simple point-to-point navigation (PointNav) [40] to complex object navigation (ObjectNav) where a robot locates a target object specified by category (e.g. ‘picture’) [41] or a detailed description (e.g. ‘find the bottom picture that is next to the top of stairs on level one.’) [42], [43]. Some studies explore multi-hop navigation, requiring discovery of multiple objects using category [44], [45] or multimodal cues [46]. These tasks assess a robot’s ability to find the target object through efficient and intelligent search of the environment by reasoning about semantic priors in the scene layouts [21], [47], [48]. We instead focus on object-centric instruction following, where the robot receives dense instructions on how to reach the target (e.g. ‘move forward

towards the cabinet then turn left and continue forwards until you reach the picture’). In this case the challenge is less efficient search, and more parsing the spatial relations of objects from complex language and grounding this structure to observations in the scene.

Vision-Language Navigation. Vision-and-Language Navigation (VLN) [16]–[18], unlike ObjectNav, provides natural language instructions that specify both the target object and how to reach it (e.g. ‘head upstairs and turn left. stop in the hallway.’). This task challenges a robot to interpret detailed instructions, that combine actions (‘turn’, ‘walk’), spatial directives (‘left’, ‘up’) and object or region references (‘chair’, ‘hallway’) in an unseen environment, making it much more challenging in terms of fine-grained language grounding. While existing VLN datasets do not distinguish between object-centric (‘move forward to the *blue chair* and stop’) and relative positional instructions (‘move forward and stop’), we argue that these two instruction types require different reasoning capabilities and need to be studied independently. Our OC-VLN dataset focuses solely on object-centric instructions, enabling a more controlled study of object-centric instruction grounding in navigation.

A fundamental challenge in both VLN and OC-VLN is how to align dense natural language instructions to a path in the real world. Trained methods can discover this alignment directly from image observations [49]–[51] or more commonly, through leveraging map-based approaches [52]–[56]. However, these methods have struggled with sim-to-real transfer problems in the few cases where they have been run in the real world [20], [21]. Recently, much VLN research has focused on exploring the impact of large language models (LLMs) and vision-language models (VLMs) to solve VLN with zero-shot approaches [57]–[63]. Some zero-shot VLN methods even outperform trained approaches in the real world [59], [63]. Some recent methods [60], [61] construct topological maps and then use an LLM-based planner, thus relying entirely on an LLM for decision making while limiting the use of traditional navigation techniques from robotics. In contrast, we introduce a zero-shot method LIFGIF that uses an LLM not as a direct planner but instead to generate an inferred pose graph from the instruction. This serves as a prior which is gradually refined during navigation using well-established robotics techniques, allowing for a more structured and adaptive approach to instruction following.

III. DATASET

We introduce *Object-Centric VLN* (OC-VLN) dataset for the instruction-following task, where a robot is required to navigate by following fine-grained object-centric instructions to reach a target. Unlike existing datasets, VLN [16] and VLN-CE [18], OC-VLN exclusively includes instructions with objects as landmarks, i.e. object-centric instructions (e.g., ‘move forward to the *couch*, then go to the *bench* in front of you and stop on the *carpet*’).

Dataset Generation. We generate our episodes using real-world 3D scans from HM3DSem [64] in the Habitat simulator [65]. We utilize the Goat-Bench [66] dataset introduced

for the GOAT task [46] where the robot needs to navigate to a sequence of open-vocabulary objects specified via a mix of different modalities, i.e. category name, image or language description. In OC-VLN we use only one modality, i.e. language. But in contrast to the language description in Goat-Bench that describes only the target object, we generate fine-grained instructions that describe the entire route from the start to the target. We do this by prompting an LLM (GPT-4 [11]) to generate navigation instructions from a series of RGB images along the route. We specifically prompt the LLM to include objects as landmarks in the instructions. We do so in two stages – *Stage 1*: we prompt GPT-4 with the RGB images from the first and last frames of the trajectory and ask it to extract key objects; *Stage 2*: we then prompt GPT-4 with all the sequential images collected for the trajectory along with the object names from Stage 1 and ask it to generate a fine-grained object-centric instruction.

Statistics. OC-VLN contains episodes having open-vocabulary language instructions with 29 words, and 8 objects on average. We support a continuous environment and an action space similar to VLN-CE (Table I). Although we have shorter path lengths, the instructions are still longer compared to VLN-CE, indicating that our instructions have more information (object-centric) for each path.

TABLE I: **Dataset comparison.** Despite shorter path lengths, OC-VLN instructions are still long as they include object-centric information.

Dataset	Environment	Action Space	Path Length	Actions	Instr. Len
R2R	Discrete	Graph-based	10.0	5	29
RxR	Discrete	Graph-based	14.9	8	129
VLN-CE	Continuous	2DoF	11.1	56	19
OC-VLN (Ours)	Continuous	2DoF	7.3	44	29

IV. METHOD

Our LIFGIF method stems from a key insight: language instructions not only guide the robot’s navigation but also encode crucial spatial information about the environment’s layout. Even before making any observations, these instructions provide the robot with a preliminary understanding of the environment’s map, albeit with significant uncertainty. For instance, the instruction “*move forward until you see a chair*.” implies the presence of a chair somewhere along the forward direction (x-axis) relative to the robot’s current position, even if we don’t know the exact distance to the chair. By representing this spatial information as a factor graph [67], we can integrate it as a prior into a traditional factor-graph-based SLAM system. As the robot observes landmarks mentioned in the instructions, the uncertainty associated with these landmarks diminishes substantially, thus helping the robot in localizing itself within the context of the instructions during navigation. This effectively bridges the gap between linguistic guidance and spatial awareness. An overview of our method is shown in Fig. 1.

A. Inferring map prior from language instructions

We transform language instructions into a *language-inferred graph*, represented by a factor graph that encodes the prior distribution of the environment’s map derived from the linguistic input. The graph includes two types of random variable nodes: (1) *waypoint* nodes, $W = \{w_i \in \text{SE}(2)\}$ representing the inferred, yet unknown, waypoints that the robot should navigate to, and (2) *landmark* nodes, $L = \{l_j \in \mathbf{R}^2\}$ representing the unknown positions of objects that the robot is expected to observe along its path. For example, consider the instruction, “*go forward to the piano. turn right. stop at the table*”. The resulting inferred graph, depicted in Fig. 3, includes four waypoint nodes: the starting point w_0 , the waypoint at the piano w_1 , the right turn waypoint w_2 , and the final stop at the table w_3 . Additionally, there are two landmark nodes: l_0 for the piano and l_1 for the table.

The inferred graph represents the following joint distribution of waypoints and landmarks given their geometric relationships described in the instruction:

$$p(W, L|R) \propto p(R|W, L) = p(R^{ww}|W)p(R^{wl}|W, L) \quad (1)$$

where $R = R^{ww} \cup R^{wl}$ is the set of all pre-defined geometric relations from the instruction, including inter-waypoint relations $R^{ww} = \{r_{i,i+1}^{ww}\}$ and waypoint-landmark relations $R^{wl} = \{r_{ij}^{wl}\}$. The graph includes two types of factors: inter-waypoint factors $p(R^{ww}|W) = \prod_i p(r_{i,i+1}^{ww}|w_i, w_{i+1})$ and landmark-waypoint factors $p(R^{wl}|W, L) = \prod_{ij} p(r_{ij}^{wl}|w_i, l_j)$.

Inter-waypoint factors $p(r_{i,i+1}^{ww}|w_i, w_{i+1})$ capture geometric relations between consecutive waypoints based on action verbs. For “*go forward*”, the relative pose r_{01}^{ww} is modeled as a Gaussian in $\text{SE}(2)$, with mean $r_{01}^{ww} = (x > 0, y = 0, \theta = 0)$ indicating forward movement. The x component has high variance due to distance ambiguity, while y and θ have low variances. This approach extends to other actions, with means and variances derived from corresponding verbs.

Landmark-waypoint factors $p(r_{ij}^{wl}|w_i, l_j)$ represent spatial relationships between waypoints and objects mentioned in the instructions. In our example, waypoint w_1 and piano landmark l_0 are modeled as being close: $p(r_{10}^{wl}|w_1, l_0) \sim \mathcal{N}(\mathbf{0}, \Sigma)$, where zero mean indicates no offset and small Σ in the diagonal elements represent low positional uncertainty.

Instruction text to inferred graph. We leverage a Large Language Model (LLM) to transform free-form textual instructions into a *language-inferred graph*. We use GPT-4 [11] to decode the instructions into an ordered sequence of waypoints, landmarks, and their relationships via this prompt: “*You are an expert in guiding a home navigation robot. The robot wants to follow a detailed language instruction to reach a target destination. To successfully complete this task, you will break down the input ‘instruction’ to output a list of ‘waypoint’, ‘landmark’, ‘waypoint-to-waypoint transition actions’ and ‘waypoint-to-landmark spatial relationship’.*” We further provide examples to the LLM to perform in-context learning (ICL) [68]–[70]. Fig. 2 shows example outputs. Next we form the *language-inferred graph* with

the waypoint nodes (w_i) from the ‘waypoint’ list, landmark nodes (l_i) from the ‘landmark’ list, inter-waypoint factors from the ‘waypoint-to-waypoint transition actions’ and the landmark-waypoint factors from the ‘waypoint-to-landmark spatial relationship’. For both the factor types, we initialize the Gaussian with a mean displacement of 2 meters in x and y . The initial values of the mean depend on the type of transition actions and landmark-waypoint relations.

	Waypoints	Actions	Landmarks	Relations
Move forward towards the red rug. Turn right and move towards the bench. Stop near the bench.	1. starting point 2. near red rug 3. after right turn 4. near bench 5. stopping point	1 → 2 move forward 2 → 3 turn right 3 → 4 move forward 4 → 5 stop	1. red rug 2. bench	1 → 2 near 2 → 4 near
Turn around. Move towards the closet. Move past the wall clock on your left.	1. starting point 2. after turning 3. near closet 4. near wall clock 5. stopping point	1 → 2 turn around 2 → 3 move forward 3 → 4 move forward 4 → 5 stop	1. closet 2. wall clock	1 → 3 near 2 → 4 left

Fig. 2: Using an LLM we extract waypoints, landmarks, waypoint-waypoint actions and landmark-waypoint relations.

B. SLAM with inferred map prior

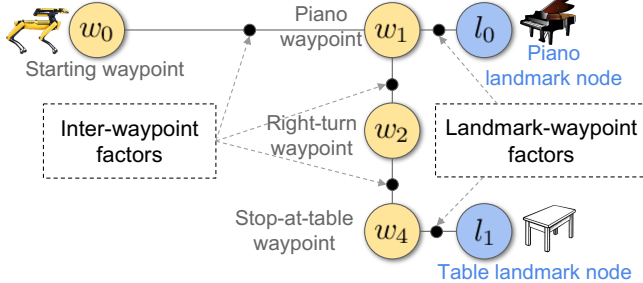


Fig. 3: **Language-inferred factor graph** corresponding to the language instruction “*Go forward to the piano. Turn right. Stop at the table*”.

Our framework integrates the language-inferred map prior into a traditional object-based SLAM navigation system. The prior map initially has high uncertainty due to the inherent ambiguity in linguistic descriptions and the lack of direct sensory information. As the robot navigates, it simultaneously localizes itself within this uncertain map while refining the map through observations, gradually transforming the vague linguistic description into a precise spatial representation.

The primary objective is to find the Maximum A Posteriori (MAP) estimate of the joint distribution over the robot poses X , observed landmarks O , language-inferred waypoints W and landmarks L , conditioned on all sensor observations Z and the linguistic descriptions of relationships among waypoints and landmarks R . Formally, this is expressed as:

$$X^*, O^*, W^*, L^* = \operatorname{argmax}_{X, O, W, L} p(X, O, W, L | Z, R)$$

which can be decomposed into two components:

$$p(X, O, W, L | Z, R) = p(X, O | Z) p(W, L | X, Z, R)$$

The first term, $p(X, O | Z)$ is the traditional landmark-based SLAM problem, which can be efficiently solved using state-of-the-art SLAM algorithms [6], [7], [67]. The second term, $p(W, L | X, Z, R)$, incorporates the language-inferred map:

$$p(W, L | X, O, Z, R) \propto p(R | W, L) p(Z | L, X) \quad (2)$$

Here, $p(R | W, L)$ is our inferred factor graph in eq. (1), and $p(Z | L, X) = \prod_{ik} p(z_{jk} | l_j, x_k)$ are the landmark-observation likelihood factors, where z_{jk} is the observation associated with the inferred landmark l_j when the robot is at pose x_k . These factors are essential for reducing uncertainty in the inferred landmarks, subsequently enhancing the accuracy and reducing the uncertainty of the associated waypoints. The inferred graph augmented with landmark-observation factors can be efficiently optimized using standard factor graph SLAM packages, such as GTSAM [71], allowing us to integrate established SLAM solutions with our novel language-informed priors with real sensory observations.

C. Data association of inferred landmarks and observations

To create the landmark-observation factors $p(z_{jk} | l_j, x_k)$ in eq. (2), we must perform data association between the inferred landmarks and the observations. In this context, a landmark could have multiple candidate observation matches, and one observation could potentially match multiple landmarks. While this data association problem could be solved using Expectation-Maximization (EM) [72], [73] or hybrid inference on a discrete-continuous factor graph [74], we opt for a simpler approach. Our method matches landmarks with observations pairwise, selecting the best match with cosine similarity between their CLIP [13] text features:

$$l^* = \operatorname{argmax}_l [\operatorname{cosine_sim}(\mathcal{F}_t(l), \mathcal{F}_o(z))] \quad (3)$$

where $\mathcal{F}_t(\cdot)$ denotes the landmark features in the inferred graph, and $\mathcal{F}_o(\cdot)$ denotes the observation features. If the similarity is below a threshold no association is made. This simple approach is effective and computationally efficient, future work may explore more sophisticated data association techniques to resolve ambiguity better.

D. Navigation policy

Localizing the robot within the language-inferred graph enables us to use a straightforward navigation policy. The robot navigates by sequentially moving to inferred waypoint nodes in the graph, transitioning when within 0.5 meter of each, and stopping at the last node. However, high uncertainty in waypoint locations can lead to inaccurate navigation. In these cases, the robot should switch to exploration mode, seeking landmarks to reduce uncertainty about upcoming waypoints. To balance exploration and exploitation, we employ the following strategy for waypoint selection:

$$w^* = \operatorname{argmin}_{w_j \forall j} [||w_j \ominus x_i||^2 + \alpha \operatorname{trace}(\Lambda_{w_j})] \quad (4)$$

This equation selects the inferred waypoint w_j that minimizes two factors: the distance between the waypoint and the current robot pose ($||w_j \ominus x_i||^2$), and the uncertainty of the waypoint, represented by the trace of its information matrix

$\Lambda = \Sigma^{-1}$. The balance between these factors is controlled by the constant α .

To determine the precise navigation target, we further sample a point from the posterior distribution $p(w^*)$ within the navigable region around w^* . Initially, the posterior distributions of waypoints have high uncertainty, promoting exploration. As the robot gathers observations, uncertainty decreases, thus refining navigation targets.

V. EXPERIMENTS

Task. At each time step, the robot has access to RGB and depth images, as well as the entire language instruction and is expected to output one of four actions: *move forward*, *turn left*, *turn right* and *stop*. We use the same agent embodiment and task setting as VLN-CE [18].

Metrics. We use standard evaluation metrics for VLN [16], [75], [76]: Success Rate (SR), Success weighted by inverse Path Length (SPL), Oracle Success Rate (OSR), and normalized Dynamic-Time Warping (nDTW). The first three measure whether the robot can reach the target object, while nDTW measures how closely it can follow the instructions.

Implementation. We evaluate LIFGIF on OC-VLN in the Habitat simulator [65] in a zero-shot manner. We use a pipeline of pre-trained methods for landmark recognition. We use RAM [77] to identify objects, followed by Grounding-Dino [14] to predict bounding boxes, and finally, Segment-Anything (SAM) [15] to obtain the semantic segmentation. For the navigator, we use a PointNav policy [40] pre-trained on HM3D [78] scenes. We compare to two zero-shot baselines, a SOTA ObjectNav method adapted to our task and an LLM-based SOTA method for instruction-following:

Seq-VLFM baseline. VLFM [48] is a single-object navigation method, which we execute sequentially for all objects, extracted using GPT-4 [11], from instructions. Using BLIP-2 [79], VLFM creates value maps of likely object locations, guiding the frontier-based exploration [80] to efficiently find objects. Note that this baseline completely disregards fine-grained navigation instructions on how to reach the target.

InstructNav baseline. InstructNav [81] is a method for general navigation instruction following which evaluates on Object-Goal navigation, VLN, and demand-driven navigation tasks. InstructNav uses an LLM to break navigation instructions into a series of paired actions and landmarks. It then plans with an LLM on how to reach each landmark using a combination of value maps representing key information about the environment such as semantic information, actions, trajectory history, and intuition. While InstructNav uses LLM as a planner, our method efficiently uses LLM offline to generate inferred graphs from instructions just once.

VI. RESULTS

Benchmark results. Table II shows that LIFGIF outperforms the baseline methods on all metrics. Our performance on the nDTW metric (48%) specifically indicates that our method is able to follow instructions better than the others. This is intuitive since our method transforms the instructions into a

graph, which is then used to perform the navigation, compared to Seq-VLFM, which searches for objects mentioned in the instructions by disregarding the actions and relations encoded into them, and InstructNav, which uses LLM to directly plan over the instructions. Being able to follow the instructions also enables LIFGIF to successfully reach the target object as indicated by its performance on the SR and SPL metrics. The OSR metric reflects whether the agent has been near the target object but failed to stop. We find that all the methods achieve reasonable OSR, indicating that the objects are easy to navigate to. However, the gap between SR and OSR is smaller for LIFGIF (20%) compared to the others (42% in Seq-VLFM and 43% in InstructNav), indicating that our method is able to call the *Stop* action correctly more often. This shows that the simple and straightforward stopping criteria in LIFGIF works fairly well, although a more sophisticated stopping policy may yield improvement.

TABLE II: **Performance.** LIFGIF significantly outperforms Seq-VLFM and InstructNav on all metrics.

Method	SR	SPL	OSR	nDTW
Seq-VLFM	0.33	0.24	0.75	0.33
InstructNav	0.24	0.07	0.67	0.33
LIFGIF (Ours)	0.58	0.40	0.78	0.48

Qualitative analysis. In Fig. 4, we visualize our agent performance on a single episode over time. At the beginning of the episode ($t = 1$), when the agent has not yet made observations in the world, the landmark nodes, $l_i = \{l_1 = \text{"brown couch"}, l_2 = \text{"fireplace"}\}$ and the waypoint nodes, $w_i = \{w_2, w_3\}$ have large uncertainties (visualized as ellipses). As the episode progresses, the agent makes observation and grounds l_1 and w_1 , thereby becoming certain about their locations. At $t = 50$, the agent observes l_2 , thus reducing uncertainty for all the nodes in the inferred graph. Finally, the agent generates the *Stop* action when it is within 0.5m of the last waypoint w_2 in the graph. To compare LIFGIF and Seq-VLFM, we visualize the agent trajectories for different episodes (Fig. 5) and observe that LIFGIF follows the instruction better compared to Seq-VLFM. This is evident from how closely the agent path matches the ground-truth path in our method.

Ablations. We perform ablations on the different modules in LIFGIF (Table III) to understand the contribution of each. For both *Object Detector* and *Navigator*, we find using an Oracle performs the best, as is expected. The Oracle detector+navigator achieves a +12% increase in success, +13% increase in SPL, and +10% increase in nDTW, indicating that the performance of our method is limited by the choice of the detector and the navigator and can be improved further.

Failure analysis. We note two main failure cases: (a) the presence of multiple instances of the same object category; and (b) the misclassification of an object. In the first case, an instruction ‘move through an open door’ in the presence of multiple doors (Fig. 6) makes it difficult for the agent to figure out the correct ‘door’. The second case is a limitation

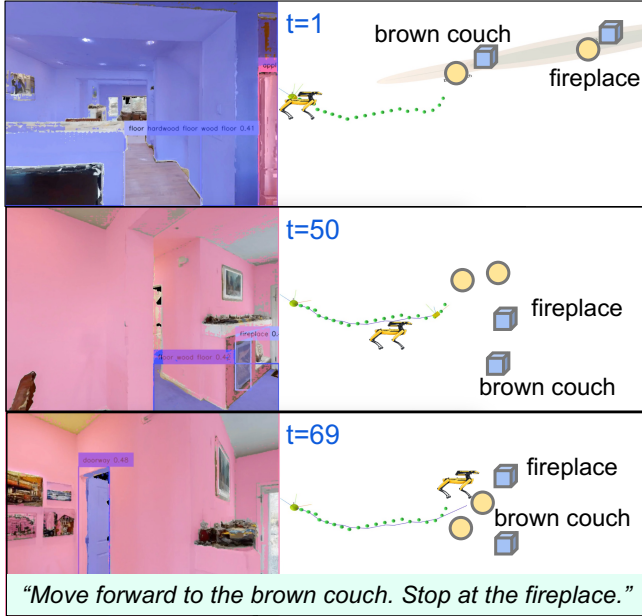


Fig. 4: **LIFGIF in action.** Visualizing the progress of our agent through an episode shows how the *language-inferred graph* gets optimized over time t by making observations in the real-world and performing data association, leading to a successful completion. (left) shows detected objects; (right) shows current robot pose, ground-truth trajectory (green), inferred waypoints (yellow) and landmarks (blue).

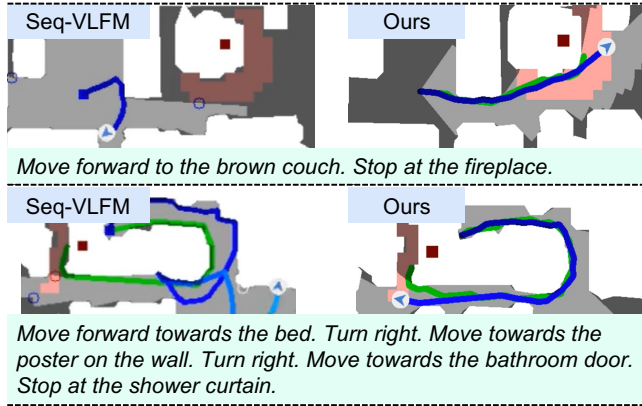


Fig. 5: **Comparison.** Our agent (right) trajectory aligns with the ground-truth trajectory better than Seq-VLFM (left), indicating better instruction following ability. Agent trajectory is **blue**, ground-truth path is **green** and target object is **red**.

of the object detector where it incorrectly identifies a ‘television’ as ‘fireplace’, leading to erroneous data association. **Real-world demonstrations.** We deployed LIFGIF on a Spot robot from Boston Dynamics to demonstrate its effectiveness in the real world. We replaced the PointNav policy with the Boston Dynamics Spot SDK as the navigator to move the robot to a waypoint. We use RTAB-Map to obtain the robot’s coordinates and the observations in a reference frame. Instead of our object detection pipeline, we use YOLOv7 [82] for faster real-time execution. We ran LIFGIF in an office space with commonly occurring objects

TABLE III: **Ablations.** Oracle versions of the *Object Detector* and the *Navigator* perform better than the pre-trained models, indicating the scope of improvement for LIFGIF.

Object Detector	Navigator	SR	SPL	OSR	nDTW
Oracle	Oracle	0.70	0.53	0.80	0.58
RAM+GDino+SAM	Oracle	0.67	0.48	0.80	0.53
RAM+GDino+SAM	PointNav	0.58	0.40	0.78	0.48

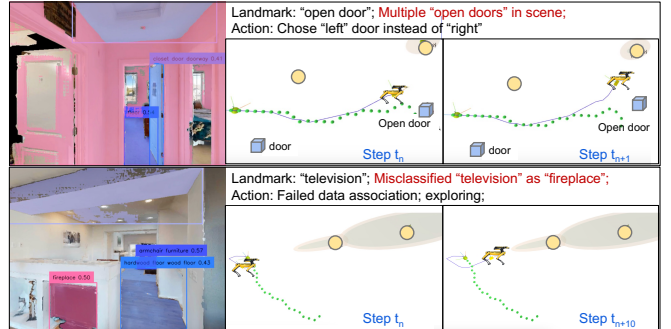


Fig. 6: **Failure cases.** Two frequent failure cases in LIFGIF are: (top) multiple instances of the same landmark present, e.g. ‘door’; and (bottom) an object is mis-classified e.g. ‘television’ identified as ‘fireplace’.

such as chairs, tables, potted plants, etc., and demonstrated that our method was able to perform well in this task.

VII. CONCLUSION

We introduce the OC-VLN dataset to study the distinct challenge of object-centric instruction following. Additionally, we propose LIFGIF, which robustly grounds dense language instructions in unseen visual environments, while navigating in a zero-shot manner. We achieve this via a combination of LLM-based technique and traditional navigation techniques from robotics. Moreover, compared to prior works that use LLM as a planner, we use it much more efficiently to generate inferred graph from language instructions offline and use the widely used factor-graph based SLAM to gradually optimize the graph during navigation. We demonstrate through experiments that LIFGIF outperforms two zero-shot state-of-the-art baselines across all metrics.

We find that LIFGIF can struggle to identify the relevant object in the presence of multiple objects of the same class. Future work in this direction could explore backtracking strategies to recover from such failures. Actively selecting poses to obtain multiple good views of the object, perhaps drawing inspiration from active SLAM, could be another avenue for future investigation to address the other significant cause of failure in LIFGIF, i.e. object misclassification.

While object-centric vision-and-language navigation is far from solved as a distinct problem, future work in this area should also explore including other distinctive environmental aspects such as regions as landmarks in the instructions, making the task more challenging.

REFERENCES

[1] S. Thrun and M. Montemerlo, “The graph slam algorithm with applications to large-scale mapping of urban structures,” *The International Journal of Robotics Research*, vol. 25, no. 5-6, pp. 403–429, 2006.

[2] R. Mur-Artal and J. D. Tardós, “Orb-slam2: An open-source slam system for monocular, stereo, and rgb-d cameras,” *IEEE transactions on robotics*, vol. 33, no. 5, pp. 1255–1262, 2017.

[3] C. Campos, R. Elvira, J. J. G. Rodríguez, J. M. Montiel, and J. D. Tardós, “Orb-slam3: An accurate open-source library for visual, visual-inertial, and multimap slam,” *IEEE Transactions on Robotics*, vol. 37, no. 6, pp. 1874–1890, 2021.

[4] A. Rosinol, M. Abate, Y. Chang, and L. Carlone, “Kimera: an open-source library for real-time metric-semantic localization and mapping,” in *ICRA*. IEEE, 2020, pp. 1689–1696.

[5] A. Rosinol, A. Violette, M. Abate, N. Hughes, Y. Chang, J. Shi, A. Gupta, and L. Carlone, “Kimera: From SLAM to spatial perception with 3D dynamic scene graphs,” *The International Journal of Robotics Research*, vol. 40, no. 12-14, pp. 1510–1546, 2021.

[6] M. Labb   and F. Michaud, “Rtab-map as an open-source lidar and visual simultaneous localization and mapping library for large-scale and long-term online operation,” *Journal of field robotics*, vol. 36, no. 2, pp. 416–446, 2019.

[7] J. A. Placed, J. Strader, H. Carrillo, N. Atanasov, V. Indelman, L. Carlone, and J. A. Castellanos, “A survey on active simultaneous localization and mapping: State of the art and new frontiers,” *IEEE Transactions on Robotics*, vol. 39, no. 3, pp. 1686–1705, 2023.

[8] W. Knight, “With a roomba capable of navigation, irobot eyes advanced home robots,” *MIT Technology Review*, 2015.

[9] E. Eade, P. Fong, and M. E. Munich, “Monocular graph slam with complexity reduction,” in *2010 IEEE/RSJ International Conference on Intelligent Robots and Systems*. IEEE, 2010, pp. 3017–3024.

[10] E. Ackerman, “Exyn brings level 4 autonomy to drones,” *IEEE Spectrum*, 2021.

[11] OpenAI, “Gpt-4 technical report,” 2023.

[12] J. Li, D. Li, S. Savarese, and S. Hoi, “BLIP-2: bootstrapping language-image pre-training with frozen image encoders and large language models,” in *ICML*, 2023.

[13] A. Radford, J. W. Kim, C. Hallacy, A. Ramesh, G. Goh, S. Agarwal, G. Sastry, A. Askell, P. Mishkin, J. Clark, *et al.*, “Learning transferable visual models from natural language supervision,” in *ICML*. PMLR, 2021, pp. 8748–8763.

[14] S. Liu, Z. Zeng, T. Ren, F. Li, H. Zhang, J. Yang, C. Li, J. Yang, H. Su, J. Zhu, *et al.*, “Grounding dino: Marrying dino with grounded pre-training for open-set object detection,” *arXiv preprint arXiv:2303.05499*, 2023.

[15] A. Kirillov, E. Mintun, N. Ravi, H. Mao, C. Rolland, L. Gustafson, T. Xiao, S. Whitehead, A. C. Berg, W.-Y. Lo, *et al.*, “Segment anything,” *arXiv preprint arXiv:2304.02643*, 2023.

[16] P. Anderson, Q. Wu, D. Teney, J. Bruce, M. Johnson, N. S  nderhauf, I. Reid, S. Gould, and A. Van Den Hengel, “Vision-and-language navigation: Interpreting visually-grounded navigation instructions in real environments,” in *CVPR*, 2018, pp. 3674–3683.

[17] A. Ku, P. Anderson, R. Patel, E. Ie, and J. Baldridge, “Room-Across-Room: Multilingual vision-and-language navigation with dense spatiotemporal grounding,” 2020.

[18] J. Krantz, E. Wijmans, A. Majumdar, D. Batra, and S. Lee, “Beyond the nav-graph: Vision-and-language navigation in continuous environments,” in *Computer Vision–ECCV 2020: 16th European Conference, Glasgow, UK, August 23–28, 2020, Proceedings, Part XXVIII 16*. Springer, 2020, pp. 104–120.

[19] A. Chang, A. Dai, T. Funkhouser, M. Halber, M. Niessner, M. Savva, S. Song, A. Zeng, and Y. Zhang, “Matterport3d: Learning from rgb-d data in indoor environments,” *Intl. Conf. on 3D Comput. Vis.*, 2017.

[20] P. Anderson, A. Shrivastava, J. Truong, A. Majumdar, D. Parikh, D. Batra, and S. Lee, “Sim-to-real transfer for vision-and-language navigation,” in *Conference on Robot Learning*. PMLR, 2021, pp. 671–681.

[21] T. Gervet, S. Chintala, D. Batra, J. Malik, and D. S. Chaplot, “Navigating to objects in the real world,” *Science Robotics*, vol. 8, no. 79, p. eadf6991, 2023.

[22] K. Jatavallabhula, A. Kuwajerwala, Q. Gu, M. Obama, T. Chen, S. Li, G. Iyer, S. Saryazdi, N. Keetha, A. Tewari, J. Tenenbaum, C. de Melo, M. Krishna, L. Paull, F. Shkurti, and A. Torralba, “Conceptfusion: Open-set multimodal 3d mapping,” *Robotics: Science and Systems (RSS)*, 2023.

[23] S. Peng, K. Genova, C. M. Jiang, A. Tagliasacchi, M. Pollefeys, and T. Funkhouser, “Openscene: 3d scene understanding with open vocabularies,” in *CVPR*, 2023.

[24] J. Zhang, R. Dong, and K. Ma, “Clip-fo3d: Learning free open-world 3d scene representations from 2d dense clip,” in *ICCV*, 2023, pp. 2048–2059.

[25] B. Chen, F. Xia, B. Ichter, K. Rao, K. Gopalakrishnan, M. S. Ryoo, A. Stone, and D. Kappler, “Open-vocabulary queryable scene representations for real world planning,” in *ICRA*. IEEE, 2023, pp. 11 509–11 522.

[26] V. Tschernezki, I. Laina, D. Larlus, and A. Vedaldi, “Neural feature fusion fields: 3d distillation of self-supervised 2d image representations,” in *2022 International Conference on 3D Vision (3DV)*. IEEE, 2022, pp. 443–453.

[27] S. Kobayashi, E. Matsumoto, and V. Sitzmann, “Decomposing nerf for editing via feature field distillation,” *Advances in Neural Information Processing Systems*, vol. 35, pp. 23 311–23 330, 2022.

[28] N. M. M. Shafullah, C. Paxton, L. Pinto, S. Chintala, and A. Szlam, “Clip-fields: Weakly supervised semantic fields for robotic memory,” in *Conference on Robot Learning Workshops*, 2022.

[29] N. Tsagkas, O. Mac Aodha, and C. X. Lu, “VL-Fields: Towards language-grounded neural implicit spatial representations,” in *International Conference on Robotics and Automation Workshops*, 2023.

[30] J. Kerr, C. M. Kim, K. Goldberg, A. Kanazawa, and M. Tancik, “LeRF: Language embedded radiance fields,” in *ICCV*, 2023, pp. 19 729–19 739.

[31] C. Huang, O. Mees, A. Zeng, and W. Burgard, “Audio visual language maps for robot navigation,” in *International Symposium on Experimental Robotics*. Springer, 2023, pp. 105–117.

[32] W. Shen, G. Yang, A. Yu, J. Wong, L. P. Kaelbling, and P. Isola, “Distilled feature fields enable few-shot language-guided manipulation,” in *Conference on Robot Learning*, 2023.

[33] F. Engelmann, F. Manhardt, M. Niemeyer, K. Tateno, M. Pollefeys, and F. Tombari, “OpenNeRF: Open Set 3D Neural Scene Segmentation with Pixel-Wise Features and Rendered Novel Views,” in *International Conference on Learning Representations*, 2024.

[34] K. Mazur, E. Sucar, and A. J. Davison, “Feature-realistic neural fusion for real-time, open set scene understanding,” in *ICRA*. IEEE, 2023, pp. 8201–8207.

[35] R.-Z. Qiu, Y. Hu, G. Yang, Y. Song, Y. Fu, J. Ye, J. Mu, R. Yang, N. Atanasov, S. Scherer, and X. Wang, “Learning generalizable feature fields for mobile manipulation,” *arXiv preprint arXiv:2403.07563*, 2024.

[36] J.-C. Shi, M. Wang, H.-B. Duan, and S.-H. Guan, “Language embedded 3D Gaussians for open-vocabulary scene understanding,” in *CVPR*, 2024, pp. 5333–5343.

[37] K. Yamazaki, T. Hanyu, K. Vo, T. Pham, M. Tran, G. Doretto, A. Nguyen, and N. Le, “Open-fusion: Real-time open-vocabulary 3D mapping and queryable scene representation,” in *ICRA*. IEEE, 2024, pp. 9411–9417.

[38] Q. Gu, A. Kuwajerwala, S. Morin, K. M. Jatavallabhula, B. Sen, A. Agarwal, C. Rivera, W. Paul, K. Ellis, R. Chellappa, *et al.*, “Conceptgraphs: Open-vocabulary 3d scene graphs for perception and planning,” in *ICRA*. IEEE, 2024, pp. 5021–5028.

[39] S. Koch, N. Vaskevicius, M. Colosi, P. Hermosilla, and T. Ropinski, “Open3DSG: Open-vocabulary 3D scene graphs from point clouds with queryable objects and open-set relationships,” in *CVPR*, June 2024.

[40] E. Wijmans, A. Kadian, A. Morcos, S. Lee, I. Essa, D. Parikh, M. Savva, and D. Batra, “Dd-ppo: Learning near-perfect pointgoal navigators from 2.5 billion frames,” in *International Conference on Learning Representations*.

[41] D. Batra, A. Gokaslan, A. Kembhavi, O. Maksymets, R. Mottaghi, M. Savva, A. Toshev, and E. Wijmans, “ObjectNav Revisited: On Evaluation of Embodied Agents Navigating to Objects,” *arXiv preprint arXiv:2006.13171*, 2020.

[42] Y. Qi, Q. Wu, P. Anderson, X. Wang, W. Y. Wang, C. Shen, and A. v. d. Hengel, “Reverie: Remote embodied visual referring expression in real indoor environments,” in *CVPR*, 2020, pp. 9982–9991.

[43] F. Zhu, X. Liang, Y. Zhu, Q. Yu, X. Chang, and X. Liang, “Soon: Scenario oriented object navigation with graph-based exploration,” in *CVPR*, 2021, pp. 12 689–12 699.

[44] S. Wani, S. Patel, U. Jain, A. Chang, and M. Savva, “MultiON: Benchmarking Semantic Map Memory using Multi-Object Navigation,” *NeurIPS*, vol. 33, pp. 9700–9712, 2020.

[45] S. Raychaudhuri, T. Campari, U. Jain, M. Savva, and A. X. Chang, “Mopa: Modular object navigation with pointgoal agents,” in *Proceedings of the IEEE/CVF Winter Conference on Applications of Computer Vision*, 2024, pp. 5763–5773.

[46] M. Chang, T. Gervet, M. Khanna, S. Yenamandra, D. Shah, S. Y. Min, K. Shah, C. Paxton, S. Gupta, D. Batra, *et al.*, “Goat: Go to any thing,” *Robotics: Science and Systems (RSS)*, 2024.

[47] D. S. Chaplot, D. P. Gandhi, A. Gupta, and R. R. Salakhutdinov, “Object goal navigation using goal-oriented semantic exploration,” *Advances in Neural Information Processing Systems*, vol. 33, pp. 4247–4258, 2020.

[48] N. Yokoyama, S. Ha, D. Batra, J. Wang, and B. Bucher, “Vlfm: Vision-language frontier maps for zero-shot semantic navigation,” *ICRA*, 2024.

[49] A. Majumdar, A. Shrivastava, S. Lee, P. Anderson, D. Parikh, and D. Batra, “Improving vision-and-language navigation with image-text pairs from the web,” in *Computer Vision–ECCV 2020: 16th European Conference, Glasgow, UK, August 23–28, 2020, Proceedings, Part VI 16*. Springer, 2020, pp. 259–274.

[50] S. Raychaudhuri, S. Wani, S. Patel, U. Jain, and A. Chang, “Language-Aligned Waypoint (LAW) Supervision for Vision-and-Language Navigation in Continuous Environments,” in *Proceedings of the 2021 Conference on Empirical Methods in Natural Language Processing*, 2021, pp. 4018–4028.

[51] J. Krantz, A. Gokaslan, D. Batra, S. Lee, and O. Maksymets, “Waypoint models for instruction-guided navigation in continuous environments,” in *ICCV*, 2021, pp. 15 162–15 171.

[52] S. Chen, P.-L. Guhur, M. Tapaswi, C. Schmid, and I. Laptev, “Think global, act local: Dual-scale graph transformer for vision-and-language navigation,” in *CVPR*, 2022, pp. 16 537–16 547.

[53] Z. Wang, X. Li, J. Yang, Y. Liu, and S. Jiang, “Gridmm: Grid memory map for vision-and-language navigation,” in *ICCV*, 2023, pp. 15 625–15 636.

[54] D. An, Y. Qi, Y. Li, Y. Huang, L. Wang, T. Tan, and J. Shao, “Bevbert: Multimodal map pre-training for language-guided navigation,” in *ICCV*, 2023, pp. 2737–2748.

[55] G. Georgakis, K. Schmeckpeper, K. Wanchoo, S. Dan, E. Miltakaki, D. Roth, and K. Daniilidis, “Cross-modal map learning for vision and language navigation,” in *CVPR*, 2022, pp. 15 460–15 470.

[56] R. Liu, W. Wang, and Y. Yang, “Volumetric environment representation for vision-language navigation,” in *CVPR*, 2024, pp. 16 317–16 328.

[57] V. S. Dorbala, G. A. Sigurdsson, J. Thomason, R. Piramuthu, and G. S. Sukhatme, “CLIP-nav: Using CLIP for zero-shot vision-and-language navigation,” 2022.

[58] G. Zhou, Y. Hong, and Q. Wu, “Navgpt: Explicit reasoning in vision-and-language navigation with large language models,” vol. 38, no. 7, pp. 7641–7649, 2024.

[59] Y. Long, X. Li, W. Cai, and H. Dong, “Discuss before moving: Visual language navigation via multi-expert discussions,” pp. 17 380–17 387, 2024.

[60] J. Chen, B. Lin, R. Xu, Z. Chai, X. Liang, and K.-Y. K. Wong, “Mapgpt: Map-guided prompting with adaptive path planning for vision-and-language navigation,” in *Proceedings of the 62nd Annual Meeting of the Association for Computational Linguistics*, 2024.

[61] Z. Zhan, L. Yu, S. Yu, and G. Tan, “Mc-gpt: Empowering vision-and-language navigation with memory map and reasoning chains,” *arXiv preprint arXiv:2405.10620*, 2024.

[62] C. Huang, O. Mees, A. Zeng, and W. Burgard, “Visual language maps for robot navigation,” in *ICRA*. IEEE, 2023, pp. 10 608–10 615.

[63] C. Xu, H. T. Nguyen, C. Amato, and L. Wong, “Vision and language navigation in the real world via online visual language mapping,” in *2nd Workshop on Language and Robot Learning: Language as Grounding*, 2023.

[64] K. Yadav, R. Ramrakhya, S. K. Ramakrishnan, T. Gervet, J. Turner, A. Gokaslan, N. Maestre, A. X. Chang, D. Batra, M. Savva, *et al.*, “Habitat-matterport 3d semantics dataset,” in *CVPR*, 2023, pp. 4927–4936.

[65] M. Savva, A. Kadian, O. Maksymets, Y. Zhao, E. Wijmans, B. Jain, J. Straub, J. Liu, V. Koltun, J. Malik, *et al.*, “Habitat: A platform for embodied ai research,” in *ICCV*, 2019, pp. 9339–9347.

[66] M. Khanna, R. Ramrakhya, G. Chhablani, S. Yenamandra, T. Gervet, M. Chang, Z. Kira, D. S. Chaplot, D. Batra, and R. Mottaghi, “Goat-bench: A benchmark for multi-modal lifelong navigation,” in *CVPR*, 2024, pp. 16 373–16 383.

[67] F. Dellaert, M. Kaess, *et al.*, “Factor graphs for robot perception,” *Foundations and Trends® in Robotics*, vol. 6, no. 1-2, pp. 1–139, 2017.

[68] T. Brown, B. Mann, N. Ryder, M. Subbiah, J. D. Kaplan, P. Dhariwal, A. Neelakantan, P. Shyam, G. Sastry, A. Askell, *et al.*, “Language models are few-shot learners,” *Advances in neural information processing systems*, vol. 33, pp. 1877–1901, 2020.

[69] J. Liu, D. Shen, Y. Zhang, B. Dolan, L. Carin, and W. Chen, “What Makes Good In-Context Examples for GPT-3?” *arXiv preprint arXiv:2101.06804*, 2021.

[70] Z. Wu, Y. Wang, J. Ye, and L. Kong, “Self-Adaptive In-Context Learning: An Information Compression Perspective for In-Context Example Selection and Ordering,” in *The 61st Annual Meeting of the Association for Computational Linguistics (09/07/2023–14/07/2023, Toronto, Canada)*, 2023.

[71] F. Dellaert and G. Contributors, “borglab/gtsam,” May 2022. [Online]. Available: <https://github.com/borglab/gtsam>

[72] F. Dellaert, S. Seitz, S. Thrun, and C. Thorpe, “Feature correspondence: A markov chain monte carlo approach,” *Advances in Neural Information Processing Systems*, vol. 13, 2000.

[73] S. L. Bowman, N. Atanasov, K. Daniilidis, and G. J. Pappas, “Probabilistic data association for semantic slam,” in *ICRA*. IEEE, 2017, pp. 1722–1729.

[74] K. J. Doherty, Z. Lu, K. Singh, and J. J. Leonard, “Discrete-continuous smoothing and mapping,” *IEEE Robotics and Automation Letters*, vol. 7, no. 4, pp. 12 395–12 402, 2022.

[75] P. Anderson, A. Chang, D. S. Chaplot, A. Dosovitskiy, S. Gupta, V. Koltun, J. Kosecka, J. Malik, R. Mottaghi, and M. Savva, “On evaluation of embodied navigation agents,” *arXiv preprint arXiv:1807.06757*, 2018.

[76] G. Ilharco, V. Jain, A. Ku, E. Ie, and J. Baldridge, “General evaluation for instruction conditioned navigation using dynamic time warping,” *arXiv preprint arXiv:1907.05446*, 2019.

[77] Y. Zhang, X. Huang, J. Ma, Z. Li, Z. Luo, Y. Xie, Y. Qin, T. Luo, Y. Li, S. Liu, *et al.*, “Recognize anything: A strong image tagging model,” in *CVPR*, 2024, pp. 1724–1732.

[78] S. K. Ramakrishnan, A. Gokaslan, E. Wijmans, O. Maksymets, A. Clegg, J. M. Turner, E. Undersander, W. Galuba, A. Westbury, A. X. Chang, M. Savva, Y. Zhao, and D. Batra, “Habitat-matterport 3D dataset (HM3d): 1000 large-scale 3D environments for embodied AI,” in *NeurIPS Datasets and Benchmarks Track (Round 2)*, 2021.

[79] J. Li, D. Li, S. Savarese, and S. Hoi, “Blip-2: Bootstrapping language-image pre-training with frozen image encoders and large language models,” in *ICML*. PMLR, 2023, pp. 19 730–19 742.

[80] B. Yamauchi, “A frontier-based approach for autonomous exploration,” in *Proceedings 1997 IEEE International Symposium on Computational Intelligence in Robotics and Automation CIRA'97. Towards New Computational Principles for Robotics and Automation*. IEEE, 1997, pp. 146–151.

[81] Y. Long, W. Cai, H. Wang, G. Zhan, and H. Dong, “Instructnav: Zero-shot system for generic instruction navigation in unexplored environment,” *CoRL*, 2024.

[82] C.-Y. Wang, A. Bochkovskiy, and H.-Y. M. Liao, “Yolov7: Trainable bag-of-freebies sets new state-of-the-art for real-time object detectors,” in *CVPR*, 2023, pp. 7464–7475.